



Topological bimeronic beams

YIJIE SHEN

Optoelectronics Research Centre, University of Southampton, Southampton SO17 1BJ, UK (y.shen@soton.ac.uk)

Received 12 May 2021; revised 28 June 2021; accepted 29 June 2021; posted 29 June 2021 (Doc. ID 431122); published 29 July 2021

This Letter proposes a family of structured light, called bimeronic beams, that characterize topological structures of bimeron (the quasiparticle homeomorphic to skyrmion). The polarization Stokes vectors of bimeronic beams emulate bimeron structures, which are reconfigurable to form various topological textures by tuning mode parameters. The bimeronic beams unveil a mechanism to transform diverse topological states of light, similar to the skyrmionic transformations among Néel, Bloch, and anti-skyrmion types. Moreover, bimeronic transformations are more generalized to include skyrmionic transformations as special cases. © 2021 Optical Society of America

<https://doi.org/10.1364/OL.431122>

Optical quasiparticles, which use optical field to emulate quasi-particle properties from particle physics and condensed matter, are potential research directions attracting growing attention as they enable new dimensions to control structured light and light–matter interactions [1–3]. They include optical skyrmions with sophisticated vectorial structures and topological protections, which were first generated in a structured electric field of evanescent wave [4], and then subsequently constructed by the spin vectors of confined freespace waves [5,6], Stokes vectors of paraxial vector beams [7,8], magnetic vectors in ultrafast pulses [9], and pseudospins in photonic crystals [10]. These optical skyrmions promise advanced applications such as nanometer- and femtosecond-scale metrology [3], deep-subwavelength microscopy [5], ultrafast vector imaging [11], and topological Hall devices [10], broadening the frontier of modern fundamental and applied physics. The beauty and success of optical skyrmions have inspired a great endeavor to explore more kinds of optical quasiparticles with generalized topological states. For instance, skyrmioniums with multi-twist topologies were recently controlled on metasurface plasmons [12], and meron structures were reported in plasmonic field [3] and optical microcavities [13], respectively. Bimerons and bimeroniums are important quasiparticles recently discovered in magnetic materials, which possess robust topological textures homeomorphic to skyrmions and offer promising features for advanced information processing, transport, and storage [14–16]. However, an optical bimeron has never been reported, to the best of the author’s knowledge.

In this Letter, a new quasiparticle state of light, optical bimeron(ium), is constructed by a family of structured vector beams. The bimeronic beams possess bimeron-like structures in their Stokes vector fields, which can be transformed to diverse

generalized topological textures, including all the intermediate skyrmionic states among Néel, Bloch, and anti-skyrmion types as simple members. A graphical model is proposed to universally represent the complete topological evolution of tunable bimeronic beams onto a 3D Poincaré-like sphere. Finally, the propagation dynamics of bimeronic beams is discussed.

Topological properties of a quasiparticle configuration can be characterized by the skyrmion number [1]:

$$s = \frac{1}{4\pi} \iint_{\sigma} \mathbf{n} \cdot \left(\frac{\partial \mathbf{n}}{\partial x} \times \frac{\partial \mathbf{n}}{\partial y} \right) dx dy, \quad (1)$$

where $\mathbf{n}(x, y) = \mathbf{n}(r \cos \phi, r \sin \phi)$ means the vector field to construct a quasiparticle confined in region σ . The skyrmion number counts how many times the vectors wrap around a unit sphere, with longitude and latitude angles noted as (α, β) . For an example of $s = 1$, shown in Fig. 1(a), the sets of vectors from skyrmion center to boundary are mapped onto the spiny sphere from the south to north pole, accordingly. Bimeron, a topological transition state of skyrmion, can also be described by the unit sphere mapping, but by changing a wrapping style, as exemplified in Fig. 1(b) for the fixed spiny sphere and skyrmion number, the coordinates of longitude and latitude are switched. Tuning the longitude and latitude coordinates with a fixed spiny sphere will have the same effect as tilting the sphere with fixed longitude and latitude lines, because the two operations are relative motions. Based on the mapping, the quasiparticle vectors can be given by $\mathbf{n} = (\cos \alpha(\phi) \sin \beta(r), \sin \alpha(\phi) \sin \beta(r), \cos \beta(r))$, and the skyrmion number can be separated into additional topological numbers:

$$\begin{aligned} s &= \frac{1}{4\pi} \int_0^{r_\sigma} dr \int_0^{2\pi} d\phi \frac{d\beta(r)}{dr} \frac{d\alpha(\phi)}{d\phi} \sin \beta(r) \\ &= \frac{1}{4\pi} [\cos \beta(r)]_{r=0}^{r=r_\sigma} [\alpha(\phi)]_{\phi=0}^{\phi=2\pi} = p \cdot m. \end{aligned} \quad (2)$$

The polarity, $p = \frac{1}{2}[\cos \beta(r)]_{r=0}^{r=r_\sigma}$, means that the vector direction is down (up) at center $r = 0$ and up (down) at boundary $r \rightarrow r_\sigma$ for $p = 1$ ($p = -1$), and the vorticity, $m = \frac{1}{2\pi} [\alpha(\phi)]_{\phi=0}^{\phi=2\pi}$, controls transverse vector components. For distinguishing diverse helical distributions, an initial phase γ should be added: $\alpha(\phi) = m\phi + \gamma$. These topological numbers provide a classic zoology of skyrmions. For the case of $m = 1$, the skyrmions of $\gamma = 0$ and $\gamma = \pi$ are classified as the *Néel type* with a hedgehog texture around the quasiparticle texture, and skyrmions of $\gamma = \pm\pi/2$ are the *Bloch type* with a vortex around the center, while the case of $m = -1$ is always

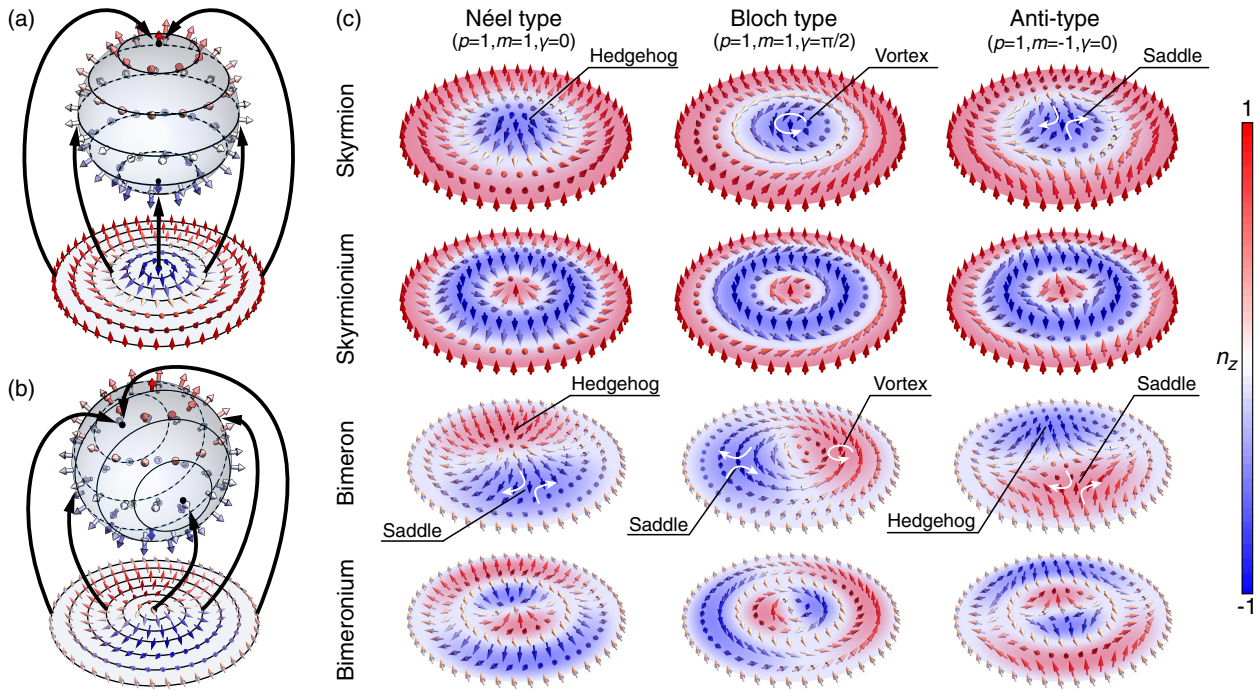


Fig. 1. (a),(b) Representations of unit sphere mapping for skyrmion and bimeron, where the gray-gradient circles mark the latitude lines set on unit spheres and the sets of vectors of quasiparticle to map correspondingly. (c) Quasiparticle zoo accommodating skyrmions, skyrmioniums, bimerons, and bimeroniums with their topological classifications as Néel, Bloch, and anti-types.

defined as *anti-skyrmion* with a saddle texture. See the first row of Fig. 1(c). In addition to skyrmions, recently, many new members have emerged in quasiparticle family with important roles [1]. An immediate derivative of skyrmion is the skyrmionium, a coupled state of two decomposed skyrmions with opposite polarities, or more decomposed skyrmions showing radially multi-twist configuration (also named target skyrmion) [12], which can also be classified as Néel, Bloch, and anti-types. See the second row of Fig. 1(c). The bimeron, as a generalized topologically transformed state of skyrmion, has the texture composed by two half-skyrmions (merons) with opposite polarities [15], where the prior topological zoology is also applicable. The third row of Fig. 1(c) shows three topological bimerons, parallel to the three topological skyrmions. The Néel-type bimeron holds a hedgehog polarity-up meron and saddle polarity-down meron, the Bloch-bimeron an up-vortex and a down-saddle, and the anti-bimeron an up-saddle and a down-hedgehog. Recently, a new concept of bimeronium was proposed as a bimeron derivative [16], akin to the skyrmionium evolved from skyrmion. Similarly, a topological zoology of bimeronium is shown in the fourth row of Fig. 1(c).

Optical skyrmions have been constructed recently by the polarization Stokes vector fields of a set of customized vector beams, namely skyrmionic beams, which are given by [7]

$$|\Psi(\mathbf{r})\rangle = LG_{0,0}(\mathbf{r})|R\rangle + e^{i\theta}LG_{0,1}(\mathbf{r})|L\rangle, \quad (3)$$

where $\mathbf{r} = (x, y, z)$, (x, y) represent transverse plane coordinates, z is a longitudinal coordinate, $LG_{n,\ell}$ is the Laguerre–Gaussian mode with radial and azimuthal indices (n, ℓ) , $|R\rangle$ and $|L\rangle$ are the states of right- and left-handed circular polarizations, and the phase θ decides the topological texture of optical skyrmion. A skyrmionic beam possesses a spatial

distribution of Stokes vectors $\mathbf{s} = (s_1, s_2, s_3)$ at focus ($z = 0$), which has a skyrmionic texture that can be controlled as the Néel ($\theta = 0$ or π) and Bloch ($\theta = \pm\pi/2$) types, but excluding anti-skyrmion. Here, a generalization is proposed to include anti-skyrmion as a special case:

$$|\Psi(\mathbf{r})\rangle = LG_{0,0}(\mathbf{r})|R\rangle + OAM(\mathbf{r}|\theta, \varphi)|L\rangle, \quad (4)$$

where the $|L\rangle$ component is replaced by the orbital angular momentum (OAM) Poincaré sphere beam, parameterized by the longitude and latitude (θ, φ) of Poincaré sphere [17]:

$$OAM(\mathbf{r}|\theta, \varphi) = \cos \varphi e^{i\theta} LG_{0,1}(\mathbf{r}) + \sin \varphi LG_{0,-1}(\mathbf{r}). \quad (5)$$

The prior skyrmionic beams, Eq. (3), are accommodated by Eq. (4) as special cases of $\varphi = 0$. The cases of $\varphi = \pm\pi/2$ correspond to anti-skyrmion, but this form still cannot represent bimeronic cases. A further generalization is proposed to this end:

$$|\Psi(\mathbf{r})\rangle = LG_{0,0}(\mathbf{r})|R\rangle + OAM(\mathbf{r}|\theta, \varphi)|\psi\rangle, \quad (6)$$

where, in contrast to Eq. (4), the left-handed polarization is replaced by an arbitrary polarization:

$$|\psi\rangle = \cos \delta e^{i\epsilon}|R\rangle + \sin \delta |L\rangle, \quad (7)$$

which, for $\delta = \pi/4$ and $\epsilon = 0$, is reduced to horizontal polarization $|\psi\rangle = |H\rangle$. When $\delta = \pi/2$ and $\epsilon = 0$ ($|\psi\rangle = |L\rangle$), Eq. (6) is reduced to the skyrmionic beam form of Eq. (4). When $\delta = \epsilon = 0$ ($|\psi\rangle = |R\rangle$), Eq. (6) is reduced to a scalar beam without quasiparticle texture. When δ ranges between 0 and $\pi/4$, Eq. (6) represents a general topological bimeronic beam. The right-upper part of Fig. 2 shows the typical topological states of the bimeronic beams with the distributions of polarization and Stokes vector, respectively.

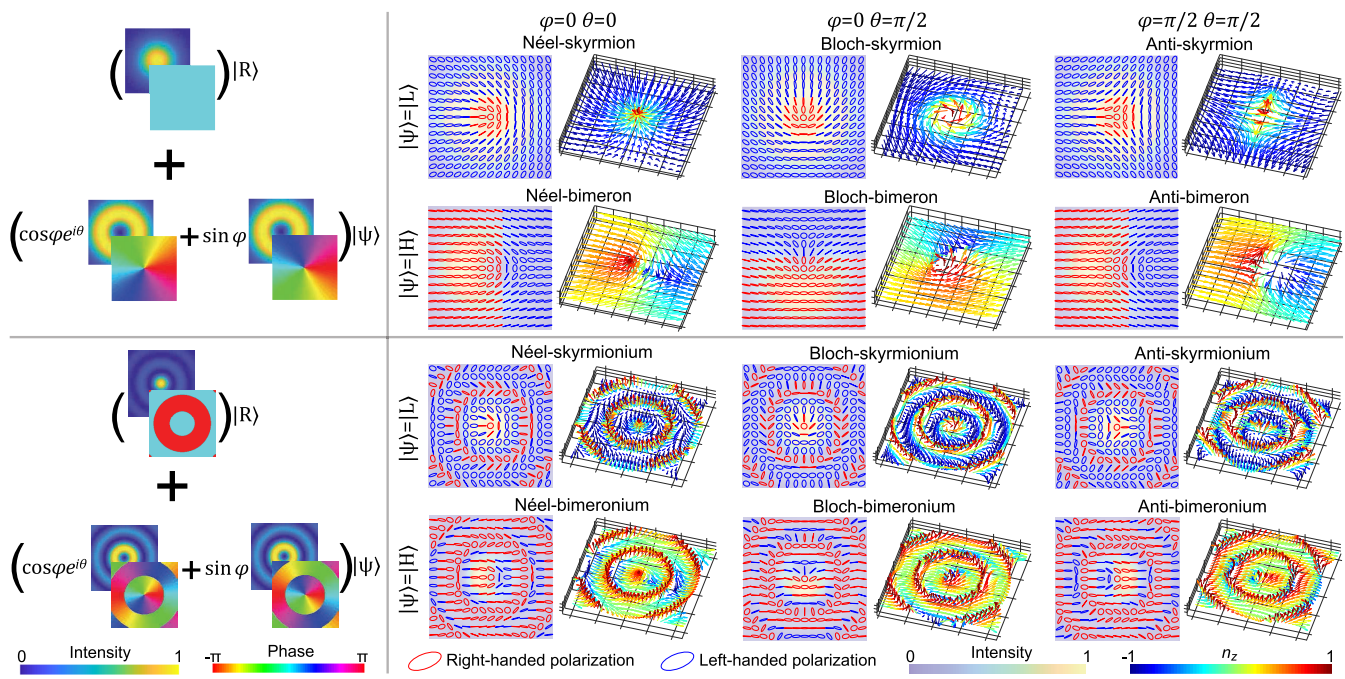


Fig. 2. Left: the conceptual structured light construction of bimeronic and bimerionomic beams with decomposed LG and Bessel modes respectively; right: the distributions of intensity, polarization, and Stokes vector at focus plane of bimeronic and bimerionomic beams, classified by various topological states as Néel, Bloch, and anti-types, with parameters noted correspondingly.

The model of bimeronic beams can be easily generalized further to include the cases of bimeronium and skyrmionium. To this end, we can exploit the LG _{$n,\pm 1$} modes with increasing radial index ($n \geq 1$) or Bessel beams [18], which have same OAM effects and also hold a unique radially multi- π -step phase structure (LG _{$n,\pm 1$} modes have n -times π -steps, Bessel mode theoretically infinite π -steps). The high-radial-index phase structure shows the evidence to be used to build the radially multi- π -twisted vector structure of bimeronium. If we replace the LG _{$0,\pm 1$} modes into high-radial-index OAM modes, the results will change into skyrmionium and bimeronium states, correspondingly (see the lower part of Fig. 2).

Hereinafter, A graphical representation to characterize the complete topological transformation of bimeronic beams is described, as shown in Fig. 3. According to the mapping of the OAM Poincaré sphere, which reveals the modal evolution from non-OAM (at equator) to pure-OAM state (at two poles), we can map the general skyrmionic beams, Eq. (4), onto a Poincaré-like sphere with a unit radius $\rho = 1$. The equator represents Néel- and Bloch-type skyrmions and intermediate skyrmions between them with tuned helicity. The two poles stand for two anti-skyrmions with orthogonal orientations. Other region reveals the topological transition states with skyrmion number evolution (e.g., from $s = 1$ at equator to $s = -1$ at poles; the case in Fig. 3), akin to the OAM evolution. In addition, the general bimeronic beams, Eq. (6), for a given value of δ , are mapped on an inner sphere of radius $\rho = \tan(\delta/2)$ ($0 < \rho < 1$). Again, the equator represents the Néel- and Bloch-type and intermediate bimerons and the poles anti-bimerons. The center of sphere, $\rho = 0$, reveals the non-quasiparticle scalar field. Then all points in the solid sphere are mapped to bimeronic beams completely, and an arbitrary route in the sphere reveals a topological transformation of the general bimeron. Such a

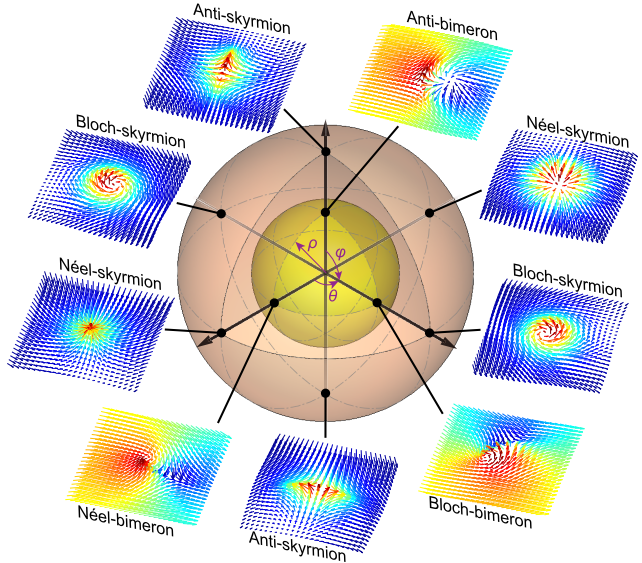


Fig. 3. Mapping of bimeronic beams onto a 3D Poincaré-like sphere, which shows complete transformations among bimerons with diverse topological textures: typical skyrmions and bimerons on selected points are shown.

3D Poincaré-like sphere for bimeronic beams provides not only a vivid understanding of its topology, but also a potential toolkit to study deeper properties of geometric phase and spin-to-orbital conversion in the future.

The propagation of a skyrmionic beam was studied, which shows a Bloch-type texture can evolve into a Néel type upon its propagation [7]. Here, similar topology-dependent propagation dynamics in bimeronic beams is shown. The result of a

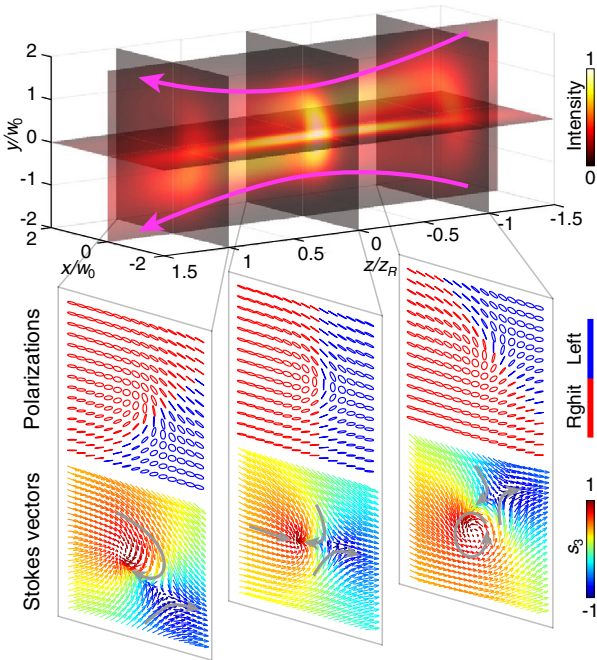


Fig. 4. Propagation dynamics of a bimerionic beam: the vector texture evolves from the Bloch to Néel type when the beam propagates through the Rayleigh range. The patterns of polarization and Stokes vector are plotted at the three propagation distances, $z = 0$ and $z = \pm z_R$, of the beam, respectively.

bimerionic beam ($\varphi = \theta = 0$, $\delta = \pi/4$) is illustrated in Fig. 4, with spatial patterns of intensity, polarization, and Stokes vector at propagation distances, $z = 0$ (at focus) and $z = \pm z_R$ (Rayleigh range). The bimerionic texture evolves from a Bloch type ($z = -z_R$), into a Néel type at focus, then gradually into an intermediate state ($z = +z_R$). When a Gaussian beam propagates through the Rayleigh range, an additional Guoy phase shift occurs, $\vartheta = \tan^{-1}(z/z_R)$, but for higher-order LG _{n,ℓ} modes, the phase shift will be stronger as $(1 + 2n + |\ell|)\vartheta$ [19]. Thus, a bimerionic beam, constructed by a Gaussian beam and a LG beam with different polarizations, will undergo a propagation-dependent phase difference between the two polarized components, which induces the longitudinal-variant vector patterns (see further discussions in Supplement). Such 3D vector patterns of bimerionic beams with elegant topological characterization meet the urgently demanded techniques for higher-dimensional structured light control [20,21].

In addition, we can further exploit the OAM modes with a larger azimuthal index (ℓ) to explore higher-order skyrmionic or bimeronic structures. Furthermore, recent advancements in structured light have promised many novel kinds of multi-singularity OAM modes [19], being a resource for creating complex optical quasiparticles, as the forms such as skyrmion bag [22], meron lattices [23], and Hopfions [24]. Recently, a multiplexing digital hologram system was proposed to generate arbitrary vector beams [25]. Therefore, the experimental generation of bimeronic beams is expected to be realized in the near future.

In conclusion, to the best of the author's knowledge, the first optical analog of bimeron is presented by a family of customized vector beams (bimeronic beams) in this Letter. The topological textures of bimeronic beams can be transformed into diverse

Néel, Bloch, and anti-types, accommodating prior skyrmionic topologies as simple members. The complete topological transformation can be represented by a 3D Poincaré-like sphere. The new topological state of light introduces extended quasiparticle methodologies into structured light control with more degrees of freedom. It opens new dimensions for information processing and light–matter interaction.

Acknowledgment. The author thanks Xichao Zhang and Ziyu Zhan for useful discussions.

Disclosures. The author declares no conflicts of interest.

Data Availability. Data underlying the results presented in this paper are available in Ref. [26].

Supplemental document. See Supplement 1 for supporting content.

REFERENCES

- B. Göbel, I. Mertig, and O. A. Tretiakov, *Phys. Rep.* **895**, 1 (2021).
- N. Rivera and I. Kaminer, *Nat. Rev. Phys.* **2**, 538 (2020).
- Y. Dai, Z. Zhou, A. Ghosh, R. S. Mong, A. Kubo, C.-B. Huang, and H. Petek, *Nature* **588**, 616 (2020).
- S. Tsesses, E. Ostrovsky, K. Cohen, B. Gjonaj, N. Lindner, and G. Bartal, *Science* **361**, 993 (2018).
- L. Du, A. Yang, A. V. Zayats, and X. Yuan, *Nat. Phys.* **15**, 650 (2019).
- R. Gutiérrez-Cuevas and E. Pisanty, *J. Opt.* **23**, 024004 (2021).
- S. Gao, F. C. Speirits, F. Castellucci, S. Franke-Arnold, S. M. Barnett, and J. B. Götte, *Phys. Rev. A* **102**, 053513 (2020).
- W. Lin, Y. Ota, Y. Arakawa, and S. Iwamoto, *Phys. Rev. Res.* **3**, 023055 (2021).
- Y. Shen, Y. Hou, N. Papasimakis, and N. I. Zheludev, "Supertoroidal light pulses: Propagating electromagnetic skyrmions in free space," arXiv:2103.08431 (2021).
- A. Karniel, S. Tsesses, G. Bartal, and A. Arie, *Nat. Commun.* **12**, 1092 (2021).
- T. J. Davis, D. Janoschka, P. Dreher, B. Frank, F.-J. Heringdorf, and H. Giessen, *Science* **368**, eaba6415 (2020).
- Z.-L. Deng, T. Shi, A. Krasnok, X. Li, and A. Alù, "Observation of topologically robust localized magnetic plasmon skyrmions," arXiv:2104.02908 (2021).
- M. Król, H. Sigurdsson, K. Rechcińska, P. Oliwa, K. Tyszka, W. Bardyszewski, A. Opala, M. Matuszewski, P. Morawiak, R. Mazur, W. Piecik, P. Kula, P. Lagoudakis, B. Pietka, and J. Szczytko, *Optica* **8**, 255 (2021).
- B. Göbel, A. Mook, J. Henk, I. Mertig, and O. A. Tretiakov, *Phys. Rev. B* **99**, 060407 (2019).
- H. Jani, J.-C. Lin, J. Chen, J. Harrison, F. Maccherozzi, J. Schad, S. Prakash, C.-B. Eom, A. Ariando, T. Venkatesan, and P. Radaelli, *Nature* **590**, 74 (2021).
- X. Zhang, J. Xia, M. Ezawa, O. A. Tretiakov, H. T. Diep, G. Zhao, X. Liu, and Y. Zhou, *Appl. Phys. Lett.* **118**, 052411 (2021).
- Y. Shen, Z. Wang, X. Fu, D. Naidoo, and A. Forbes, *Phys. Rev. A* **102**, 031501 (2020).
- O. C. Vicente and C. Caloz, *Optica* **8**, 451 (2021).
- Y. Shen, X. Wang, Z. Xie, C. Min, X. Fu, Q. Liu, M. Gong, and X. Yuan, *Light Sci. Appl.* **8**, 90 (2019).
- A. Forbes, M. Oliveira, and M. Dennis, *Nat. Photonics* **15**, 253 (2021).
- Y. Shen, I. Nape, X. Yang, X. Fu, M. Gong, D. Naidoo, and A. Forbes, *Light Sci. Appl.* **10**, 50 (2021).
- D. Foster, C. Kind, P. J. Ackerman, J.-S. B. Tai, M. R. Dennis, and I. I. Smalyukh, *Nat. Phys.* **15**, 655 (2019).
- Y. Wang, Y. Feng, Y. Zhu, Y. Tang, L. Yang, M. Zou, W. Geng, M. Han, X. Guo, B. Wu, and X. Ma, *Nat. Mater.* **19**, 881 (2020).
- I. Luk'Yanchuk, Y. Tikhonov, A. Razumnyaya, and V. Vinokur, *Nat. Commun.* **11**, 2433 (2020).
- C. Guzmán, X.-B. Hu, A. Selyem, P. M. Acosta, S. F. Arnold, R. R. Garcia, and A. Forbes, *Sci. Rep.* **10**, 10434 (2020).
- Y. Shen, "Dataset for Topological bimeronic beams," University of Southampton, 2021, <https://dx.doi.org/10.5258/SOTON/D1897>.